Orientational order in the molecular solids N_2, CO, and O_2 investigated via combined excitations with FTIR

M. Vetter,[1] A. P. Brodyanski,[1,2] S. A. Medvedev,[1,3] and H. J. Jodl[1,4]
[1]*Fachbereich Physik, Universität Kaiserslautern, Erwin Schrödinger Strasse, D-67663 Kaiserslautern, Germany*
[2]*IFOS, Insitut für Oberflächen- und Schichtanalytik, Universität Kaiserslautern, Erwin Schrödinger Strasse, D-67663 Kaiserslautern, Germany*
[3]*National Technical University, Kharkov Polytechnical Institute, 21, Frunze Strasse, 61002 Kharkov, Ukraine*
[4]*LENS, European Laboratory for Non Linear Spectroscopy, Largo E. Fermi 2, I-50125 Firenze, Italy*
(Received 4 October 2006; revised manuscript received 21 November 2006; published 23 January 2007)

We present results of studies of very weak absorption bands in the mid infrared (IR), lying in the overtone region, of solid N_2, CO, O_2, and a N_2-CO mixture. The IR activity is induced in a molecule when two neighboring molecules interact and vibrate out of phase simultaneously: (0-1)(0-1) excitation. From the temperature dependence of band intensities and bandwidths, we were able to evaluate quantitative measures of order/disorder phenomena, i.e., long range orientational ordering and/or short range correlation between molecules. The long range order parameter for ordered phases, which we determined by optical spectroscopy, agrees with values $\eta(T)$ found by x-ray Bragg scattering or nuclear quadrupole resonance data. We were able to model the temperature dependence of the order parameter by assuming a specific interaction of neighboring molecules (dipole-dipole, quadrupole-quadrupole, magnetic) and/or correlation between molecules.

DOI: 10.1103/PhysRevB.75.014305 PACS number(s): 63.20.Pw, 78.30.−j

I. INTRODUCTION

Molecular solids comprised of simple diatomic molecules, such as H_2, N_2, O_2, and CO, are studied by several experimental techniques (optical spectroscopy, structural analysis, thermal measurements, etc.) and their structure and dynamics are well modeled theoretically.[1,2] Routine investigations focus, by suitable techniques (Raman scattering, FTIR, optical spectroscopy), on fundamental excitations such as rotations/librations and translations as phonons, vibrons, and excitons, and their combinations with lattice phonons.[3] By contrast, overtone excitations in solids (e.g., molecular vibrations $v=0\rightarrow 2,3,4,\ldots$) are much less studied because they are much weaker than the fundamental one ($v=0\rightarrow 1$); intensities are smaller by 10^{-2} to 10^{-4}. These combined excitations in the ordered solid can be either localized in one molecule [i.e., $(0\rightarrow 2)$ vibron as a whole crystal excitation, called bivibron] or delocalized on two neighboring molecules [i.e., (0-1)(0-1) vibron as a whole crystal excitation, called two-vibron]. It is expected that this process fulfils symmetry requirements, that these two molecules are interacting strongly, and that they are well oriented to each other. Therefore, spectral fingerprints, such as band shape, intensity, and width, of these combined excitations will provide information directly about the specific intermolecular interaction and their orientational order parameter. To test our idea, one can systematically vary physical parameters and compare the resulting spectra: (i) the intermolecular interaction in α-N_2 is that of two electric quadrupole moments, whereas in α-CO the electric dipole moment plays a significant role and in α-O_2 the magnetic interaction is dominant; (ii) by raising the temperature in these pure molecular solids, one can study the transition from highly oriented ordered phases to orientationally disordered ones; and (iii) in mixtures of N_2-CO or N_2-Ar one can control the specific intermolecular interaction by controlling the impurities.

We here briefly summarize the properties of the low temperature phases of N_2, CO, and O_2, and we cite the relevant literature on theoretical models for combined excitations [the two-vibron (0-1)(0-1)]. Table I summarizes the crystallographic structure of each phase and its temperature regime, and the number of molecules per unit cell. Recent reviews[2,4] present the relevant theory for solid N_2 or solid O_2. The α-CO was experimentally studied by Legay-Sommaire and Legay (Ref. 5, and papers cited therein) and has been theoretically modeled by Zumofen.[6] The (0-1)(0-1) two-vibron region in FTIR spectra of solid N_2 has been described, with inferences for astrophysical application;[7] properties of the spectra were qualitatively explained as due to collision induced interaction. Legay-Sommaire and Legay repeated these measurements and modeled the IR absorption taking into account that these vibrational levels are excitons (see below).[8] The same combined excitations in solid CO were studied again by IR absorption by Legay-Sommaire and Legay.[5] In none of these experimental studies was there any systematic study of the temperature dependence (of band frequency, bandwidth, and band intensity) nor the transition from ordered to disordered phases; there was no report of possible higher combined excitations [e.g., in the (0-3) region] and there was no comparison of different molecular elements (N_2, CO, O_2, and mixtures).

In a separate publication, Legay and Legay-Sommaire calculated the intensity, bandwidth, and frequency of the combined excitation (0-1)(0-1) of IR absorption in α-CO.[9] In a first model the authors tried to estimate this band intensity (0-1)(0-1) in comparison to the fundamental one (0-1) by assuming the molecules interacted only via induced dipole-induced dipole moment. Their resulting theoretical value of band intensity (10^{-5}) was much smaller than the experimental value (10^{-2}). Next they took into account the possibility of a Fermi resonance between two interacting molecules (1, 2) with the following levels: $|0|2\rangle$ and $|2|0\rangle$, which means

TABLE I. Low temperature crystal structures.

Substance	Phase	T (K)	Structure	Number of molecules in unit cell
N_2	α	$\leqslant 35$	$Pa3$ (T_h^6)	4
	β	$35<T<55$	$P6_3/mmc$ (D_{6h}^4)	2 (orientationally disordered)
O_2	α	$\leqslant 24$	$C2/m$ (C_{2h}^3)	1 (structural cell) 2 (magnetic cell)
	β	$24<T<44$	$R\bar{3}m$ (D_{3d}^5)	1 (structural cell)
	γ	$44<T<55$	$Pm3n$ (O_h^3)	8 (orientationally disordered) 2 spherelike and 6 disklike molecules
CO	α	$\leqslant 61$	$P2_13$ (T^4)	4
	β	$61<T<68$	(D_{6h}^4)	2 (orientationally disordered)

molecule 1 in $v=0$ state and molecule 2 in $v=2$ (anharmonic level) and vice versa [(0-2) transition at 4252 cm^{-1}]; and $|1|1\rangle$, which means molecule 1 in $v=1$ state and simultaneously molecule 2 in $v=1$ [the (0-1)(0-1) transition at 4278 cm^{-1}]. The strength of this Fermi resonance is weaker than the classic one (ν^+, ν^- in CO_2). The theoretical ratio of integrated intensity $I_{(0\text{-}1)(0\text{-}1)}$ to $I_{(0\text{-}2)}$ was determined to be 0.012 (from experiment 0.012); there was excellent agreement between the theoretical model and the experimental results for the band position, the difference of unperturbed and perturbed levels of the Fermi resonance components, as well as the bandwidth. Indeed, the authors applied the Fermi resonance model to the free molecule case; i.e., instead of excitonic levels they used vibrational levels; they considered interacting molecules 1 and 2 but without resonance interaction in the crystal, which would deliver a vibron density of states. The agreement between theoretical results and spectral findings justifies their approach. However, Raman and IR spectra of the fundamental vibron in solid CO possess bandwidths of about 2–5 cm^{-1}. These originate from vibron density of states and not from an inhomogeneous broadening due to head-tail disorder; these bands are much broader than in α-N_2, which will be modeled next.

In addition to modeling α-CO, Legay and Legay-Sommaire modeled the two-vibron excitation in α-N_2. They used the solid state picture—as opposed to a model using only free molecules—and calculated numerically the vibron density of states (DOS) and the integrated intensity for the (0-1)(0-1) excitation.[8] For the vibron DOS, the authors solved the dynamical matrix (using standard lattice dynamics) in combination with symmetry arguments. They considered force constants between first-, second-, and third-nearest neighbors. For the integrated intensity of this excitation, the authors described the induced dipole moment by an electric quadrupole-quadrupole interaction between neighboring molecules. In both cases the numerical agreement between spectra and theory is excellent (due to many adjustable parameters). Our aim here in solid nitrogen is to improve the experiment itself (instead of condensed, annealed films measured at $T=5$ K, we use grown crystals), to study the band shape and band intensity carefully as a function of temperature (up to and within the β phase of N_2), to discuss the integrated intensity $I(T)$ in the framework of an order parameter and to apply these studies to mixtures N_2-CO [such as (0-1)(0-1) in N_2 or CO and (0-1) at N_2 molecule (0-1) at CO molecule simultaneously].

Because the (0-1)(0-1) combined excitation is a simultaneous excitation distributed among two neighboring molecules, the description of this process will depend on several factors, such as the kind of mutual intermolecular interaction, the density of states, and the relative orientation both molecules. The last factor is usually described by an order parameter, which is obviously different for the ordered and orientational disordered phases of N_2, O_2, CO, and N_2-CO mixtures. The spectral fingerprint in our studies will be the integrated intensity $I(T)$; this is expected to be proportional to the order parameter, and so it is a function of temperature.

The aim of this paper is to determine the vibron DOS and the order parameter $\eta(T)$ from spectra of N_2, CO, O_2 and mixtures. Further, we discuss the effect on these results of the intermolecular interaction and orientational ordering. In the next section, we will briefly describe the production and treatment of samples as well as our spectroscopic technique. We will present some prototype spectra to document the complexity and richness of information and the unambiguous spectral assignments. The accompanying discussion comprises two main sections: the two-vibron (0-1)(0-1) in ordered systems of α-N_2, α-CO, and α-O_2, and the combined vibration (0-1)(0-1) in disordered systems of β-N_2, β^*-N_2-CO (here we denote a special phase in a mixture with an asterisk), and γ-O_2.

II. EXPERIMENTAL PROCEDURE AND RESULTS

We used in our experiments nitrogen gas of 99.999% purity, oxygen gas of 99.998% purity, and carbon monoxide of 99.998% purity. In the case of $(N_2)_x$-$(CO)_{1-x}$ mixtures, both pure gases were premixed in a chamber to produce the desired to partial pressures. They were maintained there for several days to ensure complete mixing. We used the brass cells described in Ref. 10. To investigate the combined modes in the range 2000–6000 cm^{-1}, we used various windows: diamond windows (aperture 3 mm, sample thickness 1.1 mm), quartz windows (aperture 10 mm, sample thickness 6.7 mm), and sapphire windows (aperture 10 mm, sample thickness 5.5 or 20.5 mm). Our technique to grow big poly-

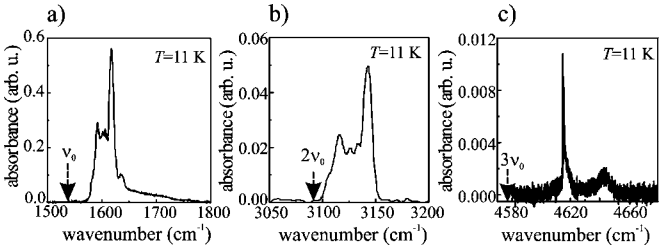

FIG. 1. Fundamental and overtone vibrational region of solid O_2 at 11 K (different scales in absorbance).

crystalline samples is described elsewhere.[3] We measured sample temperature, in the range of 10–80 K, by a calibrated silicon diode, which was directly attached to the sample cell; absolute accuracy of temperature registration was about 0.1 K. Spectra were recorded in this mid IR region by a Fourier spectrometer (Bruker 120 HR) both on cooling and warming cycles. A tungsten lamp was used as the light source, Si on CaF_2 as a beam splitter, and liquid N_2-cooled InSb as the detector (accessible range 1900–11 000 cm^{-1}). Our spectral resolution was 0.1–0.5 cm^{-1}, depending on the bandwidth of interest.

The real concentration $(N_2)_x$-$(CO)_{1-x}$ was determined as follows. First, we determined the integrated intensity of the (0-3) mode of pure CO, with sample thickness 1 mm. Second, we determined the integrated intensity of the (0-3) mode of CO in the mixtures. Considering different thicknesses (pure CO and mixture) from the intensity ratios, we determined the real concentrations to be x=91%, 59%, and 19%, with an estimated error of less than 2%. We studied three concentrations $(N_2)_{0.91}(CO)_{0.09}$, $(N_2)_{0.59}(CO)_{0.41}$, and $(N_2)_{0.19}(CO)_{0.81}$.

In this section, we will illustrate the weakness of the intensity and the richness of spectral information. Figure 1 shows the (0-1) region (~1550 cm^{-1}), (0-2) region (~3100 cm^{-1}) and (0-3) region (~4600 cm^{-1}) of the fundamental mode of solid O_2 at 11 K. Of interest here is the small scale in absorbance. In general the ratio of integrated intensities of phonon sideband to the zero phonon line (ZPL) is about 1%. Here we will discuss spectral features of the (0-1)(0-1) combined modes, which are a few percent of the respective integrated intensity of phonon sidebands. The phonon sideband to the (0-1) and (0-2) mode (see Fig. 1) is already discussed in our previous publication;[3] the (0-3) region shows no zero phonon line (ZPL) at 4578.5 cm^{-1}, but shows a broad (~70 cm^{-1}) weak phonon sideband. On top of this is a very narrow doublet at 4615 and 4615.5 cm^{-1} (see Fig. 7). Figure 2 shows the (0-2) region (ν_0~2143 cm^{-1}, $2\nu_0$~4280 cm^{-1}) of solid $(N_2)_{0.59}$-$(CO)_{0.41}$ as a function of temperature. Some spectral features (bandwidth, band shape) clearly change at the α^*-β^* CO phase transition. By referring to the literature,[11] we assign (see Fig. 2) the (0-2) overtone of $^{12}C^{18}O$, $^{13}C^{16}O$, and $^{12}C^{16}O$ as zero phonon lines (ZPL) plus phonon sideband (shaded area). The measured relative intensities $I(^{12}C^{18}O):I(^{13}C^{16}O)=1:5$ confirm natural abundance of isotopes ($^{12}C^{18}O$=0.20%, $^{13}C^{16}O$=1.10%); the peak amplitude of the main isotope is not reliable because of saturated detector signal (peak 3, Fig. 2). At higher temperatures

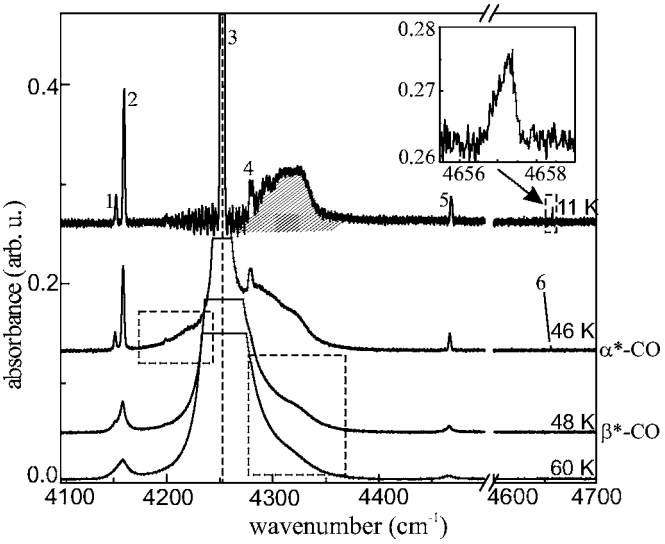

FIG. 2. Overtone region of CO in the mixture $(N_2)_{0.59}$-$(CO)_{0.41}$ as a function of temperature. Assignment: peak 1, (0-2) mode of $^{12}C^{18}O$; peak 2, (0-2) mode of $^{13}C^{16}O$; peak 3, (0-2) mode of $^{12}C^{16}O$; peak 4, (0-1)(0-1) mode of CO; peak 5, (0-1)N_2(0-1)CO mode; peak 6, (0-1)(0-1) mode of N_2; shaded area, phonon sideband to ZPL peak 3.

within α^*-CO in the mixture, we can recognize an anti-Stokes phonon sideband to the ZPL [(0-2) of $^{12}C^{16}O$]. This phonon sideband in α^*-CO is slightly structured, whereas the same sideband in β^*-CO is just a broad wing on the Stokes side of the ZPL. In α^*-CO at low temperatures the overtone (0-2) $^{12}C^{16}O$ is very narrow (Γ~5 cm^{-1}) and the band shape is fully Lorentzian, whereas in β^*-CO it is much broader (Γ~50 cm^{-1}) and has a broad Gaussian band shape. Three additional peaks (4, 5, and 6), which will be discussed later as combination modes (0-1)(0-1), are well documented in Fig. 2.

III. DISCUSSION

In the first part of this section we will discuss low temperature ordered phases. In the second part we will discuss high temperature disordered phases. In each section we will present examples of N_2, CO, $(N_2)_x$-$(CO)_{1-x}$ and O_2, as well as comparisons between them.

A. Ordered systems

1. Two-vibron band in α-N_2

Besides a phonon sideband, a narrow (full width ~1 cm^{-1}) absorption band is observed in the spectra of solid N_2 in the region of the first vibrational overtone. In Fig. 3(a), we show the temperature evolution of this band, which exists only in orientationally ordered α phase.

This band was discovered earlier and interpreted as two-vibron band.[8] Such band appears in spectra due to coupling between vibron modes possessing different symmetry A_g and T_g: $\omega_{\text{two-vib}}=\omega_{A_g}(\mathbf{k}_1)+\omega_{T_g}(\mathbf{k}_2)$ and $\mathbf{k}_1+\mathbf{k}_2=0$. The shape of the two-vibron band at our lowest experimental temperature

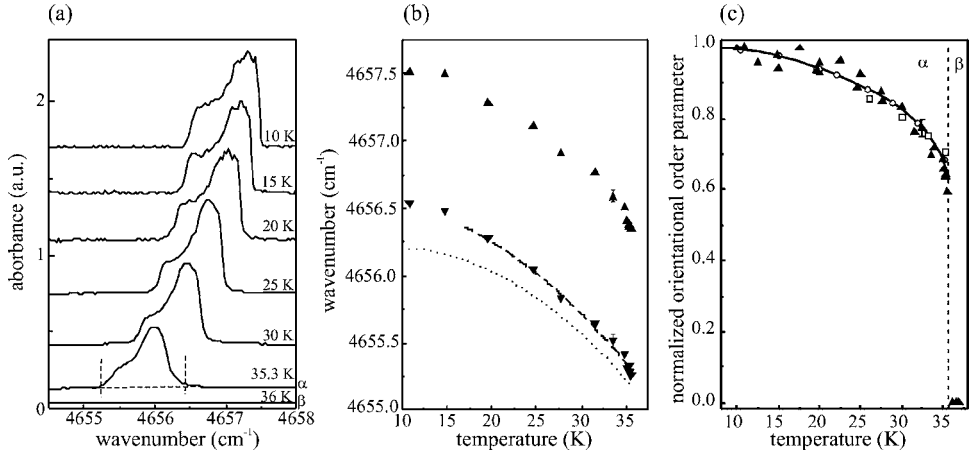

FIG. 3. (a) Two-vibron in α-N_2: (0-1)(0-1) spectra as a function of temperature during warming; (b) vibron zone as a function of temperature with low frequency border (▼) and high frequency border (▲). Combined excitation $\omega(A_g)+\omega(T_g)$ in Raman spectra as a function of temperature by Beck *et al.* (Ref. 12) [dashed (------) line] and by Quillon *et al.* (Ref. 13) [dotted (···) line]; (c) reduced integrated absorption of two-vibron band as a function of temperature (our data ▲). Orientational order parameter from nuclear quadrupole resonance studies by Scott (○ data from Ref. 3). Solid line (-) by Antsygina *et al.* on the basis of theory (Ref. 14), □, x-ray data by Strzhemechny (Ref. 15).

(10 K) is similar to that measured by Legay and Legay-Sommaire at 5 K.[8] Those authors already modeled the spectral features in detail by fitting this vibron DOS by a couple of parameters, expressing the interaction between first-, second-, and third-nearest neighbors. The position of the lower frequency border [see Fig. 3(b)] of this vibron zone is at 4656.5 cm^{-1}, which coincides exactly with the sum of $\omega_{A_g}=2327.7$ and $\omega_{T_g}=2328.8$ cm^{-1} (data from Ref. 12); the high frequency border is at 4675.5 cm^{-1}. We remeasured carefully both borders of this vibron DOS as a function of temperature [Fig. 3(b)], and we compared these with published Raman data. The width of the (0-1)(0-1) vibron zone ($\sim$1 cm^{-1}) hardly changes with changing temperature. This behavior was modeled by Legay and Legay-Sommaire for $T=0$ K by the sum of coupling constants between first- (δ) and second- (γ) nearest neighbors $\Delta=\omega(A_g+T_g)_{max}-\omega(A_g+T_g)_{min}=-16\delta-8\gamma$.

We model the intramolecular vibrations in these molecular solids as low energetic Frenkel excitons. By so doing, we can express the frequency of these excitations in a crystal in the following form:

$$\omega_{0-n}^{cr}(\mathbf{k})=\omega_{0-n}^{gas}+D_{0-n}+M_{0-n}(\mathbf{k}).$$

Here n is the vibrational quantum number, $\omega_{0-n}^{cr}(\mathbf{k})$ and ω_{0-n}^{gas} are the frequencies of the $0-n$ internal vibrational transition in the crystal and in the free molecule respectively ($\mathbf{k}$ is a wave vector of these excitations in a crystal); D_{0-n} describes the change in the energy of this transition in a single molecule because of its interaction with surrounding particles in a condensed medium (so-called an "environmental" frequency shift); $M_{0-n}(\mathbf{k})$ is the term arising due to an exchange of excitations between molecules in a crystal. This last term is responsible for the width of the vibron energy zone, usually called the "resonance" frequency shift. Applying this model and using known experimental values for D and M of α-N_2 (Ref. 3), we can calculate the width of two-vibron band as sum of "resonance" frequency shifts of T_g and A_g modes,

$$\Delta=M_{0-1}(T_g)+M_{0-1}(A_g)=0.4+0.8\sim 1.2\ \text{cm}^{-1}.$$

The experimental value deduced from Fig. 3(b) is $\Delta\sim 1$ cm^{-1}. This is in good agreement with the calculated value.

The integrated intensity of this two-vibron band decreases with increasing temperature within α-N_2 and disappears in that form in β-N_2 [Fig. 3(c)]. This is to be expected because in β-N_2 there are two orientational disordered molecules in the unit cell (Table I); these interact via another mechanism to produce local vibrations (see below).

It is known that the structure of the orientationally ordered low temperature phase of nitrogen is stabilized mainly by the electrostatic quadrupole-quadrupole interaction between neighboring molecules. Therefore, the intensity of the two-vibron band in this phase can be expressed in the following way:

$$I_{\text{two-vib}}=Q^2R^{-8}A[g(\omega_{A_g}\omega_{T_g})]\eta^2.$$

Here Q is the electrostatic quadrupole moment of the N_2 molecule, R is the distance between molecules, A is the integral of two-vibron DOS $g(\omega_{Ag}\omega_{Tg})$ over the Brillouin zone, and η is the orientational order parameter (OP). Eliminating thermal expansion, such as $R(T)$, we define the reduced integrated intensity, normalized to lowest temperature values,

$$I_{\text{two-vib}}(T)R^8(\text{T})/I_{\text{two-vib}}(10\ \text{K})R^8(10\ \text{K}),$$

which is plotted in Fig. 3(c) (our data ▲). The only experimental set of data for the OP from nuclear quadrupole resonance (NQR), investigations by Scott,[4] are in full agreement with our experimental values. Theoretical determination of $\eta(T)$ for α-N_2 [the solid line in Fig. 3(c)] by Antsygina *et al.*[14] is integrated for comparison. Later we will compare the range of OP (at $T=0$, $\eta=1$, at $T_{\alpha\beta}\eta=0.6$) and its T dependence with our results for α-CO and for $(N_2)_x-(CO)_{1-x}$ mix-

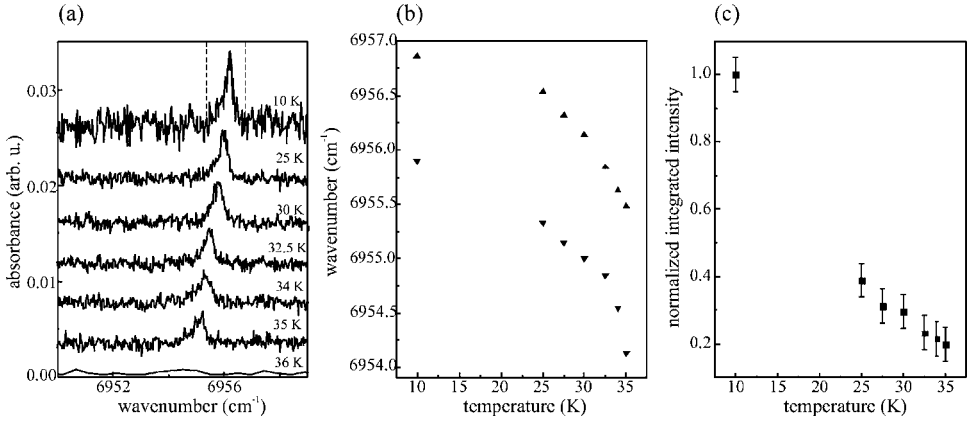

FIG. 4. Two-vibron in α-N_2: (a) spectrum as a function of temperature in α- and β-N_2. Low energy and high energy border is indicated. (b) Vibron zone as a function of temperature. (c) Normalized integrated intensity $I(T)/I(10\ \mathrm{K})$ as a function of temperature.

tures; by so doing, we will get a deeper insight into both similar but different systems, although isomorphous systems. To conclude, the spectral determination of the OP is as good as the one found by other more complicated techniques.

Very recently, Strzhemechny suggested a further method to determine the absolute value of the orientational order parameter from diffraction intensities (x-ray-Bragg scattering) and applied this technique to α-N_2.[15] We incorporate his data in Fig. 3(c), which possess a pretty large uncertainty. All these independent experimental techniques (NQR, diffraction, and optical scattering) confirm the trend of $\eta(T)$, modeled successfully by a self-consistent theory.[14]

In the spectral region of the second overtone ($\sim$6950 cm^{-1}), we discovered a very weak absorption band. Figure 4(a) shows spectra at different temperatures within α-N_2. These disappear in β-N_2. The low and high energy border of this vibron zone we plot in Fig. 4(b) as a function of temperature.

To model the position of this band at 10 K between 6955.8 and 6956.8 cm^{-1}, we use the frequency of the Raman mode A_g (2327.7 cm^{-1}) and the combination of both Raman modes A_g (2327.7 cm^{-1}) and T_g (2378.8 cm^{-1}) minus the molecule anharmonicity of the gas ($2\omega_e x_e$=27.8 cm^{-1}, Ref. 16), which delivers a combined frequency of 6956.4 cm^{-1}; in comparison to the low energy border at 6956 cm^{-1} [Fig. 4(b)]. Therefore, we assign this absorption band to a two-vibron band generated by two neighboring molecules, vibrating out of phase (IR activity) with $\omega_{A_g}^{0-1}(\mathbf{k})$ and $\omega_{A_g+T_g}^{0-2}(-\mathbf{k})$; the intermolecular interaction is like the case of the two-vibron (0-1)(0-1) via electric quadrupole-quadrupole interaction.

The band shape of the spectrum at 10 K is similar to the vibron zone of the two-vibron feature (0-1)(0-1) [Fig. 3(b)]. The temperature dependence of the low and high energy border is about $\Delta\omega$=−(1.4 to 1.8) cm^{-1}, warming up until $T_{\alpha\beta}$ (35 K). It is of the same order of magnitude as the vibron zone (0-1)(0-1), which is $\Delta\omega$=−(1.2 cm^{-1}) for temperatures below $T_{\alpha\beta}$. In comparison to the frequency shifts of the A_g and T_g modes as a function of temperature within α-N_2: $\Delta\omega$=−0.5 cm^{-1} (Fig. 4 in Ref. 3); i.e., this behavior is therefore describable by mere thermal expansion $V(T)$.

The integrated intensity scaled to the lowest temperature $I(T)/I(10\ \mathrm{K})$ is plotted in Fig. 4(c). Since important values at low temperatures are missing there, we cannot analyze and compare it with Fig. 3(c).

2. Two-vibron band in α-CO

Figure 5 displays the temperature evolution of absorption spectra of solid CO in the region of the first vibrational overtone. Besides a strong absorption line $\nu_{0\text{-}2}$ (at 4250 cm^{-1}) and a phonon sideband (shaded area), we observe a relatively weak absorption band that persists only in the orientationally ordered α phase and disappears in the β-CO ($T_{\alpha\beta}\sim$61 K).

To determine the band position, we follow either the theoretical model by Zumofen,[6] who modeled the vibron DOS of the fundamental mode, or the model by Legay and Legay-Sommaire,[9] who modeled the (0-1)(0-1) two-vibron mode using the Fermi-resonance model. In addition, other literatures offer various different values for fundamental frequencies, the value of the molecule anharmonicity constant, etc., e.g., the overtone (0-2) at 11 K in α-CO is at 4252.6 (Fig. 2). Using the best known value for the fundamental mode by IR studies,[11] 2138.46 cm^{-1}, we get an anharmonic constant $\omega_e x_e$ of 12.9 cm^{-1}; the literature offers values between 12 and 14 cm^{-1}.

Because solid N_2 and CO are isomorphous with respect to mechanical aspects as well as crystal structure, we follow the same analysis as we did for (0-1)(0-1) in α-N_2. The position of the lower frequency border [Fig. 5(c)] of this vibron zone is at 4275 cm^{-1}, which coincides roughly with the sum of ω_{A_g} 2135.5 cm^{-1} and ω_{T_g} 2138 cm^{-1} to be 4273.5 cm^{-1} (both data are from Ref. 6); the high frequency border is at 4285 cm^{-1}. If we consider only spectroscopic data from Raman scattering (maximum at 2139 cm^{-1}, bandwidth 5 cm^{-1}) and from IR absorption (maximum at 2138.5 cm^{-1}, bandwidth 2 cm^{-1}), we get as a sum frequency 4277.7 cm^{-1}, which is comparable to the maximum of the (0-1)(0-1) band at 4280 cm^{-1} [see Fig. 5(c)]. In both cases (low frequency border, band maximum) the difference between our experimental values and modeled values is about −(1.5–2.0) cm^{-1}.

According to Fig. 5(c), this vibron DOS shows a slight usual temperature behavior $[-(\Delta\omega/\omega)/\Delta T \leqslant 10^{-2}]$ during warming. This can be modeled, in general, by the mere volume expansion $V(T)$ of solid CO (e.g., for α-N_2, Fig. 4 in Ref. 3). The width of this spectral feature (0-1)(0-1) was modeled by Legay and Legay-Sommaire with a homogenous and inhomogeneous bandwidth to be $\sim$5 cm^{-1},[9] as in our spectra (5–6 cm^{-1}). We prefer instead the exciton model for the two-vibron band; Zumofen determined for the fundamental mode a width of $\sim$8 cm^{-1} (perfect structure), or $\sim$6 cm^{-1}

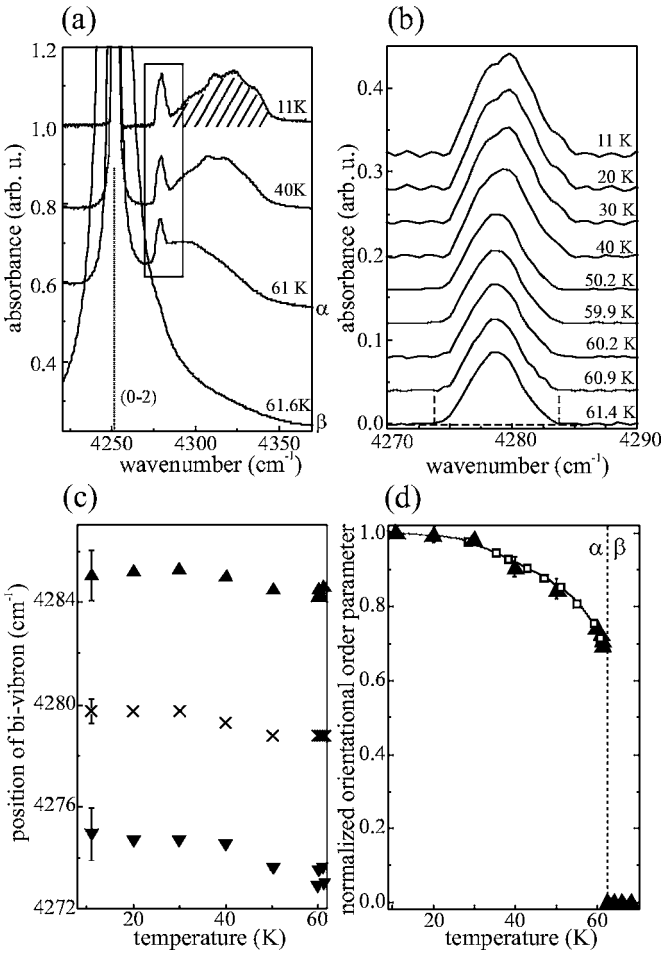

FIG. 5. Two-vibron in α-CO: (a) part of spectrum as in Fig. 2. (b) (0-1)(0-1) spectrum as a function of temperature (like peak 4 in Fig. 2). (c) Vibron zone as a function of temperature with low frequency border (▼) and high frequency border (▲); position of band maximum (x). (d) Reduced integrated absorption $I(T)/I(10\ \mathrm{K})$ of this two-vibron as a function of temperature (▲, our data); □, order parameter from nuclear quadrupole resonance studies by Scott (Ref. 17); Solid line (-) by Antsygina *et al.* on the basis of theory (Ref. 14).

including disorder;[6] these values correspond to the width of the vibron zone 10 cm^{-1} [high frequency-low frequency border in Fig. 5(c)].

At lowest temperatures, the ratio of integrated intensity $I_{(0\text{-}1)(0\text{-}1)}/I_{(0\text{-}2)}$ is about 0.03. Contrary to nitrogen, the CO molecule has a dipole moment. Therefore IR activity of the two-vibron absorption band in this substance is mainly due to the electric dipole-dipole interaction (D) and the intensity of this band can be expressed as follows:

$$I_{\text{two-vibron}}(\mathrm{CO}) = D^2 R^{-6} A[g(\omega_{A_g}\omega_{T_g})]\eta^2.$$

As for the case of N_2, we eliminate thermal expansion such as $R(T)$, and define the reduced integrated intensity normalized to lowest experimental temperature

$$I_{\text{two-vibron}}(T)R^6(T)/I_{\text{two-vibron}}(10\ \mathrm{K})R^6(10\ \mathrm{K}).$$

This is plotted in Fig. 5(d).

There is only one published set of data to describe this order parameter η in α-CO, by NQR studies,[17] Those agree with our data pretty well. Theoretical determination of η(T) for α-CO [solid line in Fig. 5(d)] by Antsygina *et al.*[14] is integrated for comparison. The range of the order parameter $\eta(T)$ will be compared with other system (N_2 and N_2-CO) and discussed later.

3. *Two-vibron bands in* N_2-CO *mixtures*

In the literature we did not find any statements about the orientational behavior of molecules in mixtures. For the N_2-CO mixture, we found only concentration-dependent Raman studies[18] and IR studies.[19] These suggest a one- and two-mode behavior. But the studies contradict each other. Especially in a system consisting out of quasi-identical molecules, one is tempted to presume that their dynamics is also identical.

In Fig. 6, we show the two-vibron spectra as a function of concentration and temperature. The $(0\text{-}1)N_2+(0\text{-}1)N_2$ two-vibron band [around 4660 cm^{-1}, Fig. 6(c)] as a function of CO concentration is smeared out and slightly shifted with respect to the one in the pure system, as expected (DOS of ordered and disordered systems). The $(0\text{-}1)\mathrm{CO}+(0\text{-}1)N_2$ two-vibron band [around 4470 cm^{-1}, Fig. 6(b)] demonstrates the effective coupling of these two vibrations of different molecules; the lower band edge in spectra is located at 4466 cm^{-1}; ω (A_g of N_2) =2327.7 cm^{-1} plus ω (IR in CO) =2138.5 cm^{-1}. An increase of CO concentration broadens this vibron zone considerably. The (0-1)CO (0-1)CO two-vibron band [around 4280 cm^{-1}, Fig. 6(a)] is clearly visible next to the intense CO overtone (0-2) and its phonon sideband [see Figs. 2 and 5(a)]. This band barely changes—only in intensity—with decreasing CO concentration [Fig. 6(a)].

The temperature dependence of these three bands (CO two-vibron, N_2-CO two-vibron, and N_2 two-vibron) at a given concentration shows dramatic differences [Figs. 6(d)–6(f)]. The frequency shift with raising temperature is almost the same for all excitations (−2 cm^{-1}/40 K), explainable by similar thermal expansion in all lattices, whereas the amplitude of the absorption band decreases by a factor 4 in the case of N_2 and by a factor of 1.3 in the case of N_2-CO and in the case of CO. This means that the specific intermolecular interaction of pairs of molecules N_2-N_2 and N_2-CO is temperature sensitive. All bands disappear at $T>54$ K (the $\alpha^*-\beta^*$ phase transition).

A better way to look at this temperature-dependent, different dynamics of N_2 and CO molecules in this mixture is given by the orientational parameter $\eta(T)$. We plot the reduced normalized order parameter for the N_2 two-vibron [Fig. 6(g)] and for the N_2-CO two-vibron [Fig. 6(h)] [raw data are ratio of integrated band intensities $I(T)/I(10\ \mathrm{K})$]. In the case of the two-vibron excitation in the pair of N_2 molecules, if CO is admixed into the pure N_2, the transition temperature $T_{\alpha\beta}$ rises from $T=35$ K to 55 K (T-c% diagram in Ref. 20). The range of the N_2 order parameter changes from $\eta=1$ (at $T=0$ K) to $\eta\sim0.6$ (at $T_{\alpha\beta}$). If CO is admixed, the change in $\Delta\eta(T)$ is smaller than in the pure case. In the

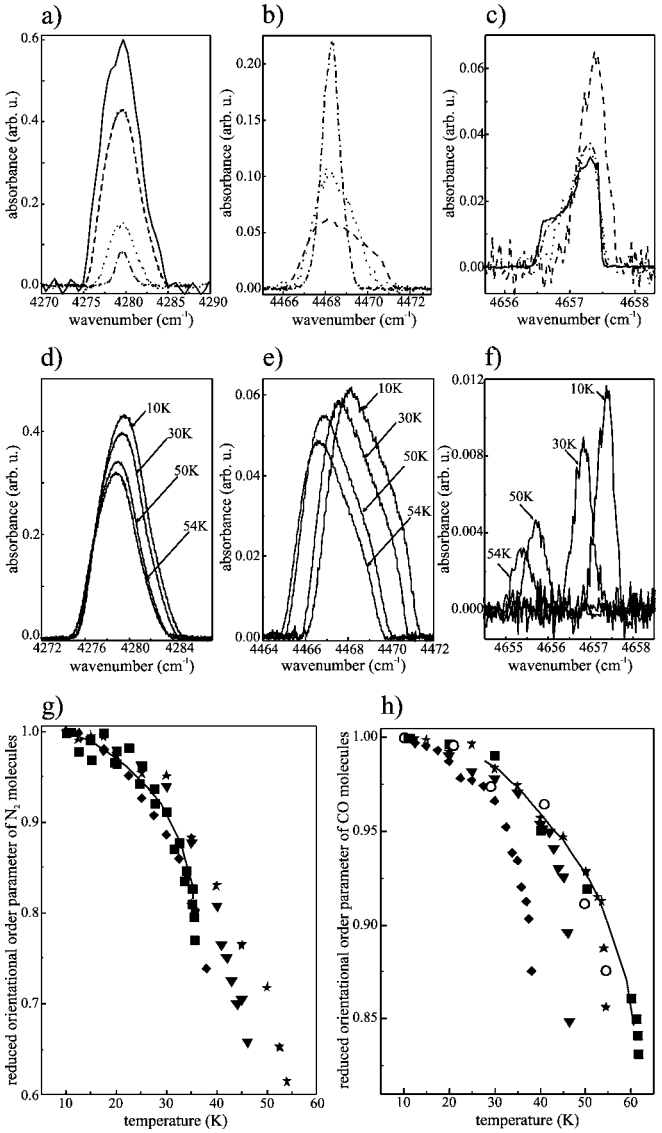

FIG. 6. Two-vibron in α^* N_2-CO mixtures: (a) (0-1)CO(0-1)CO spectrum at 10 K as a function of concentration of CO (100% solid, 81% dashed, 41% dotted, 9% dash-dotted). (b) (0-1)CO(0-1)N_2 spectrum at 10 K as a function of concentration of CO (81% dashed, 41% dotted, 9% dash-dotted). (c) (0-1)N_2(0-1)N_2 spectrum at 10 K as a function of CO concentration (81% dashed, 41% dotted, 9% dash-dotted, 0% solid). (d) (0-1)CO(0-1)CO spectrum of $(N_2)_{0.19}$-$(CO)_{0.81}$ as a function of temperature. (e) (0-1)CO(0-1)N_2 spectrum of $(N_2)_{0.19}$-$(CO)_{0.81}$ as a function of temperatures. (f) (0-1)N_2(0-1)N_2 spectrum of $(N_2)_{0.19}$-$(CO)_{0.81}$ as a function of temperatures. (g) Reduced orientational order parameter for the (0-1)N_2(0-1)N_2 excitation as a function of temperatures and different concentrations [■, pure N_2; ♦, 91% N_2; ▼, 59% N_2; ★, 19% N_2; solid line, pure N_2 as in Fig. 3(c)]. (h) Reduced orientational order parameter for the (0-1)CO(0-1)N_2 excitation as a function of temperatures and different concentrations [■, 100% CO; ★, 81% CO; ▼, 41% CO; ♦, 9% CO; solid line, pure CO as in Fig. 5(d)].

case of the N_2-CO two-vibron, if N_2 is admixed into pure CO the transition temperature, $T_{\alpha\beta}$ drops from $T=60$ K to 38 K.[20] The range of the CO order parameter changes from $\eta=1$ ($T=0$ K) to $\eta\sim0.85$ (at $T_{\alpha\beta}$). If N_2 is admixed, the change in $\Delta\eta(T)$ is larger than in the pure case.

4. Two-vibron band in α- and β-O_2

The previous discussion dealt with crystals consisting of molecules interacting via electrostatic dipole moments (CO) or quadrupole moments (N_2). Contrary to these molecules, the homonuclear molecule O_2 has zero dipole moment, and its quadrupole moment is very small compared to the N_2 molecule. At the same time, the oxygen molecule has nonzero spin, and the magnetic interaction is a relevant contribution to total energy of the crystal lattice. Due to symmetry reasons (one molecule in the unit cell), we do not observe any additional absorption bands in the spectral range of the first overtone other than phonon sidebands [Fig. 1(b)]. In the spectral region of the second overtone, we discovered a IR-active band [Fig. 7(a)], represented by a narrow doublet superposed on a weak phonon sideband to the IR inactive (0-3) fundamental at 4578.5 cm^{-1}.[2,21] Subtracting this phonon sideband [Fig. 7(b), lower panel] from the whole spectra [Fig. 7(a)], we end up with the narrow (with a total width about few wave numbers cm^{-1}) doublet [Fig. 7(b) upper panel].

The temperature dependence of this part of spectrum is presented in Fig. 7(c). These plots shows a clear change at the α-β phase transition ($\sim$24 K). In the β phase of O_2, we observe only one asymmetric band. Within a small temperature range (>1 K), both spectra are present, thereby demonstrating that this phase transition is of first order due to phase coexistence.

We interpret this narrow absorption band as a two-vibron band, i.e., a simultaneous excitation of two-vibron modes by one photon whose frequency equals the sum of the fundamental and the first overtone vibron frequencies: $\omega_{\text{two-vib}}=\omega_{0\text{-}1}(\mathbf{k}_1)+\omega_{0\text{-}2}(\mathbf{k}_2)$ and $\mathbf{k}_1+\mathbf{k}_2=0$. The largest transition dipole moment is induced when both interacting molecules vibrate out of phase. Using this assumption, we interpret the two spectral maxima of the two-vibron band in α-O_2 as due to coupling of interacting vibrons at two points in $\mathbf{k}$ space: $\mathbf{k}_1\perp\mathbf{a}$, $k_1\approx\pi/b$ and $\mathbf{k}_2\perp\mathbf{b}$, $k_2\approx\pi/a$ ($\mathbf{a}$ and $\mathbf{b}$ are vectors of the unit cell in the basal plane of α-O_2). This excitation propagates in two nonequivalent directions ($\mathbf{a}$ and $\mathbf{b}$) in the α phase (that is why we observe a doublet), and it propagates in one preferential direction in the β phase, where we observe one band only (for further details, see the crystal structure Sec. III and the magnetism Sec. VI in Ref. 2).

Using the same approach as in the case of the two-vibron band in α-N_2, we can calculate the position of this band; taking (0-1) at 1546.8 cm^{-1} and (0-2) at 3069.8 cm^{-1} both from IR data (Table II in Ref. 3), we get as a sum 4616.6 cm^{-1}. This value is close to the position of this band in α-O_2. Because dispersion of the 0-2 vibron is negligible,[3] the width of this two-vibron band mirrors the width of the fundamental density of states. The total width of this band is about 8 cm^{-1}, close to the value of the resonance frequency shift $\sim$6 cm^{-1} obtained by us earlier based on analyzing the phonon sidebands to intramolecular vibrations.[3] The dependence of the low frequencies and high frequency border of this band on temperature is presented in Fig. 7(d). The fre-

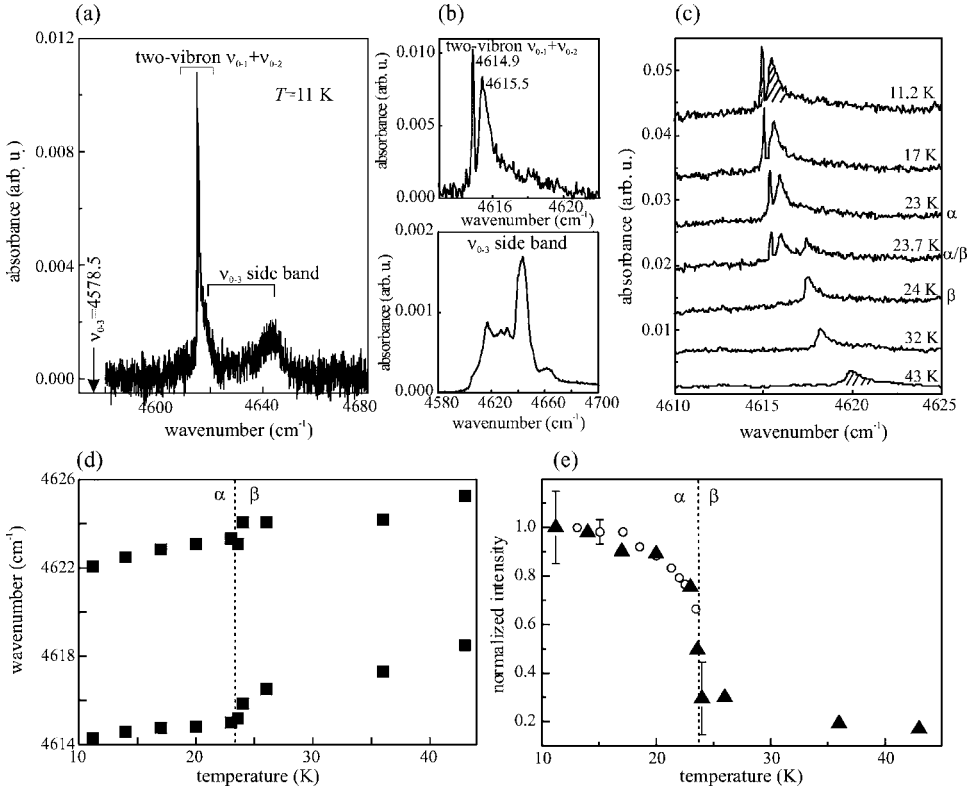

FIG. 7. Two-vibron in α- and β-O_2: (a) total spectrum at 11 K; (b) deconvolution of total spectrum into two-vibron (upper part) and phonon sideband (lower part). (c) Two-vibron part of total spectrum as a function temperature; α phase, β phase, and α-β phase coexistence is indicated. (d) Low and high frequency border of this band [Fig. 7(b), upper part] as a function of temperature in α and β phase. (e) Normalized integrated intensity $I(T)/I(11\ \mathrm{K})$ as a function of temperature in α and β phase: ▲, our data; for comparison normalized intensity of pure magnon from Ref. 22 (○).

quencies of band borders increase slightly as temperature increases. At the α-β phase transition a small jump in frequencies occurs ($\sim$0.8 cm^{-1}), in agreement with earlier reports of similar jumps in frequencies at this transition (Fig. 6 in Ref. 3).

We also observed a similar band in α-N_2 [(0-1)(0-2) in Sec. III A 1], but its integrated absorption is about two orders of magnitude weaker than the one in O_2. Because two-vibron bands in solid nitrogen borrow their intensity from electrostatic quadrupole-quadrupole interaction ($I \sim Q^2$) and because the electrostatic quadrupole moment of O_2 is very small $[(Q_{O2}/Q_{N2})^2 \approx 0.08]$, we trace the IR activity of the two-vibron band in solid O_2 back to the magnetic interaction within the basal planes. The normalized intensity of this two-vibron band in α- and β-O_2 is plotted in Fig. 7(e).

Although the uncertainty in intensity is large for this very weak band, the tendency is clearly recognizable: a decrease from the α phase during warming of the sample and a constant contribution from the β phase. Because this combined excitation is originally generated by the specific magnetic interaction of neighboring O_2 molecules, it should be interpreted in the framework of a magnetic order parameter. Therefore, we display also results of similar spectroscopic studies: the integrated intensity of the pure magnon excitation.[22] The courses of intensities of two-vibron band and magnon peak are similar in the whole temperature range of existence of α-O_2. Consequently, we conclude that the intensity of the two-vibron band reflects the long range magnetic order parameter in magnetically ordered α-phase.

5. Comparison of order parameters

We here summarize the order parameter of the two-vibron excitation for pure N_2, for pure CO, and for their mixture.

The order parameter at the α-β phase transition is $\eta \sim 0.6$ in both cases of pure solids, but this transition temperature for pure N_2 is at 35 K while the one for pure CO is at 60 K [Figs. 3(c) and 5(d)]. In mixtures, the concentration-dependent order parameter $\eta(c,T)$ describes the case between the two pure cases systematically [Figs. 6(g) and 6(h)].

Although both molecules N_2 and CO are quasi-identical (isoelectronic, isomorphous, mechanical parameters) and their mixture is characterized by perfect solubility (T-c% diagram), the orientational behavior is different for both molecules; the change in order parameter $[\eta(T=0\ \mathrm{K})=1$ to $\eta(T_{\alpha\beta}) \sim 0.6]$ is the same but the range in temperature is twice as large for CO; i.e., the CO molecules are stronger logged in than N_2 molecules. This is obviously a consequence of the intermolecular interactions producing differently high local potential barriers: for the interaction between neighboring CO molecules via electrostatic dipoles and between neighboring N_2 molecules via electrostatic quadrupole moments.

In the mixture N_2-CO, the α-β phase transition is caused by the instability of the orientational state of N_2 molecules: librations of the molecules in the α phase to librational jumps in the β phase.[23] To conclude, this difference in the dynamics of both molecules in the pure N_2 and pure CO remains even in the ideal mixture N_2-CO.

In the orientationally ordered phases of oxygen, we discovered the two-vibron band due to coupling of (0-1) and (0-2) vibrations. Since the quadrupole moment of O_2 is very small compared to that of N_2, the IR activity of this band is mainly due to the magnetic interaction between molecules. Therefore, the intensity of this band reflects the magnetic order parameter.

The bandwidth, even better the width of the basis of a spectral band, differ, a consequence of the different interactions to produce a vibron density of states. In α-N_2, the basis of the spectral band is $1-2$ cm^{-1}, and the interaction between neighboring molecules is described by an electric quadrupole-quadrupole interaction; in α-CO, the basis is $6-8$ cm^{-1}, and the interaction between neighboring molecules is similar (electric dipole-dipole) but there is an additional disorder due to head-tail disorder (CO, OC directions, dipole disordering). In α-O_2 the basis of the spectral band is $6-8$ cm^{-1} and the interaction is described by magnetic moments.

B. Disordered systems

The preceding discussion dealt with the two-vibron excitations in ordered systems. These are characterized by a narrow vibron zone ($1-2$ cm^{-1}); and a band intensity that decreases during heating and that completely disappears at the order-disorder phase transition. It is desirable to look for a similar excitation in disordered systems. These disordered systems (β-N_2 or γ-O_2) there exhibit no long range interaction, so one does not expect lattice excitations in the form of a two-vibron model. But due to local short range interaction, there might exist a (0-1)(0-1) combined simultaneous vibration near the (0-2) overtone. Because the disordered solid phases are similar to the liquid phases, we would expect this combined vibration to remain in both phases.

1. Combined vibration (0-1)(0-1) in β-N_2

We observe in β-N_2 and liquid (l) N_2 a broad absorption band near the (0-2) overtone at 4627 cm^{-1} [Fig. 8(a)]. This feature was already observed but not studied extensively;[7] in general, the induced IR activity is explained by collisions between molecules. In our studies we extended these investigations as a function of temperature and to mixtures (N_2-CO).

Because we have already studied in detail the phonon sideband to the fundamental (0-1) and (0-2), (0-3) overtones in α- and β-N_2, we know exactly this spectral shape for deconvolution of complex spectra (Fig. 3 in Ref. 3). Therefore, we are able to subtract the phonon sideband to the (0-2) vibrations from the total spectrum to get this additional broad band [shaded area in Fig. 8(b)]. Its temperature dependence is presented in Fig. 8(c). On the basis of careful studies by IR absorption and Raman scattering, we know that the form and position of the phonon sideband changes little with temperature,[3] whereas this broad band is very temperature sensitive [Fig. 8(c)].

The position of band maximum at 4654 cm^{-1} can be modeled by the Raman-active A_g mode in β-N_2 at 2326.6 cm^{-1}.[3,13] This is slightly shifted to higher frequencies during warming. The bandwidth increases enormously from $\sim$10 cm^{-1} at 36 K to about 50 cm^{-1} at 75 K; this inhomogeneous broadening is attributable to dynamic disorder (not static disorder due to crystal imperfections) as a consequence of a stronger coupling of vibrations with translations and with rotations at higher temperatures.

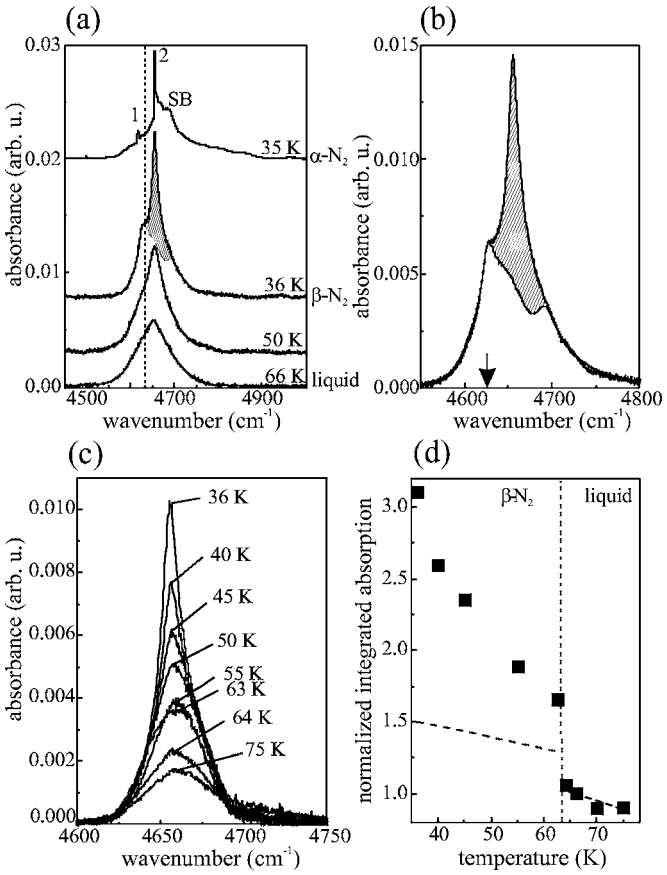

FIG. 8. (a) Combined excitation spectrum in β-N_2 as total spectrum and function of temperature (band with shaded area of interest; peak 1 is the combined excitation of (0-1)^{14}N(0-1)^{14}N^{15}N; peak 2, the two-vibron (0-1)(0-1) N_2 [see Fig. 3(a)] and phonon sideband. (b) Spectrum at 36 K consisting out of phonon sideband to (0-2) overtone and (0-1)(0-1) combined vibration (shaded area); position of (0-2) overtone at 4627 cm^{-1}. (c) Part of spectrum [shaded area of Fig. 8(b)] as a function of temperature. (d) Normalized integrated intensity $I(T)/I(66\ \mathrm{K})$ as a function of temperature in β-N_2 and l-N_2. Considering only thermal expansion, dashed line.

All these findings support the following model: in β-N_2, there exist two orientationally disordered molecules per primitive cell; neighboring molecules, interacting via electric quadrupole moments, are each simultaneously excited to the (0-1) state, vibrating out of phase; this combined excitation is a local excitation only. Because different pairs of molecules, in different geometrical relation to each other, can vibrate producing such a broad band (width $\sim$10 cm^{-1} at $T=36$ K), the resulting feature is much broader than the bandwidth of two-vibron excitations of about $1-2$ cm^{-1}, which result from inhomogeneous broadening due to static disorder.

Figure 8(d) shows the scaled integrated intensity $I(T)/I(66\ \mathrm{K})$. This decreases in the β phase and exhibits a pronounced jump at the β-l phase transition. It also decreases in l-N_2. Because the IR activity comes from the induced dipole moment in neighboring molecules, varying with distance R, interacting via electric quadrupole moment Q, we can model the IR intensity as

$$I(T) \sim Q^2 R^{-8} F(r_i r_j),$$

where $F(r_i r_j)$ is a function that describes the strength of the orientational correlation between two molecules i and j with unit vectors $\mathbf{r}_i$ and $\mathbf{r}_j$ along the molecular axes (basically a short range order parameter). In a first step, we model the thermal expansion of the crystal, as we did in Sec. III A, by $[R(T)/R(66\ \mathrm{K})]^{-8}$. This appears as a broken line in Fig. 8(d). This approach models satisfactorily the behavior in liquid phase. However, the discrepancy between experimental data points and the theoretical values (the broken line) increases as the temperature decreases in the β phase. This striking dependence of the intensity on temperature indicates that strong correlations in the orientational motion of molecules exist in this disordered phase and that these correlations strongly decrease as temperature increases. Recently Brodyanski *et al.*[3] analyzed the fundamental vibrations in orientational disordered phases of β-N_2 and found that the orientational motion of molecules along the c axes of β-N_2 structure is strongly correlated. These authors calculated the two-component short range order parameter that describes the rotational motion of molecules in β-N_2. Figure 9 (in Ref. 3) shows the temperature dependence of the two-component short range order parameter. The overall behavior is correctly described—a decrease in the order parameter raising temperature. Because our function F is represented by two components (Fig. 9 in Ref. 3) and because we do not know the weight of each component, we cannot model the strong correlation part theoretically of our experimental data [Fig. 8(d)]. It should be noted that this theory uses the fact that this intermolecular potential in β-N_2 needs an anisotropic part.

At the end of this section, we will compare this spectroscopic result $I(T)$ and its interpretation here in β-N_2 with other systems such as γ-O_2 and N_2-CO mixtures.

2. Combined vibration (0-1)(0-1) in γ-O_2

We observe a broad absorption band near the (0-2) overtone at 3070 cm^{-1}. The band shape of this feature changes drastically in the different phases α, β, γ, l-O_2 [Fig. 9(a)]. Because we know the form and position and the temperature dependence of the phonon sideband to the (0-2) overtone very accurately[3]—as in the case of β-N_2—we are able to subtract from the whole spectrum this phonon sideband and obtain a broad band [shaded area in Fig. 9(b)], whose temperature dependence is displayed in Fig. 9(c). Most striking is the change in peak amplitude as a function of temperature. By contrast, the band maximum and bandwidth ($\sim$10 cm^{-1}) change very little. The position of the band maximum is at 3102 cm^{-1}. This value can be modeled either by Raman-active modes (doublet in γ-O_2 at 1552.0 cm^{-1} and 1553.2 cm^{-1}) or by the zero phonon line in IR spectra (at 1550.5 cm^{-1}).[3] Both sets of data are slightly shifted with respect to the experimental band maximum of 3102 cm^{-1}.

To explain this IR-absorption band, we use the following model: γ-O_2 has eight molecules per unit cell; six of them are rotating in a disk (disklike, called d) and two of them are freely rotating in a sphere (spherelike, called s). Because this absorption band in γ-O_2 is about ten times stronger than the same one in β-N_2 and because the electric quadrupole moment of N_2 is much larger than that of O_2, the interaction mechanism must be different than in the case of β-N_2, namely, via magnetic moments of O_2 molecules (the spin of O_2 molecule is $S=1$). Therefore neighboring molecules, interacting magnetically, are simultaneously excited to the (0-1) state, vibrating out of phase; this combined excitation is a local excitation only. The exchange interaction J is larger between disklike molecules than between disk-sphere molecules or spherelike molecules (see Sec. VI about magnetism in solid oxygen in Ref. 2),

$$J_{dd} > J_{ds} > J_{ss}.$$

Therefore, we assume that mainly neighboring molecules within a quasi-one-dimensional chain of disklike molecules are interacting here. The possibility of orientational disorder might explain why the bandwidth ($\sim$10 cm^{-1}) in γ-O_2 is much smaller than the broader one in β-N_2.

In Fig. 9(d), we plot the scaled integrated intensity $I(T)/I(55\ \mathrm{K})$ as a function of temperature. This ratio decreases steadily during heating. The dipole transition moment M of this combined excitation, which is related to the

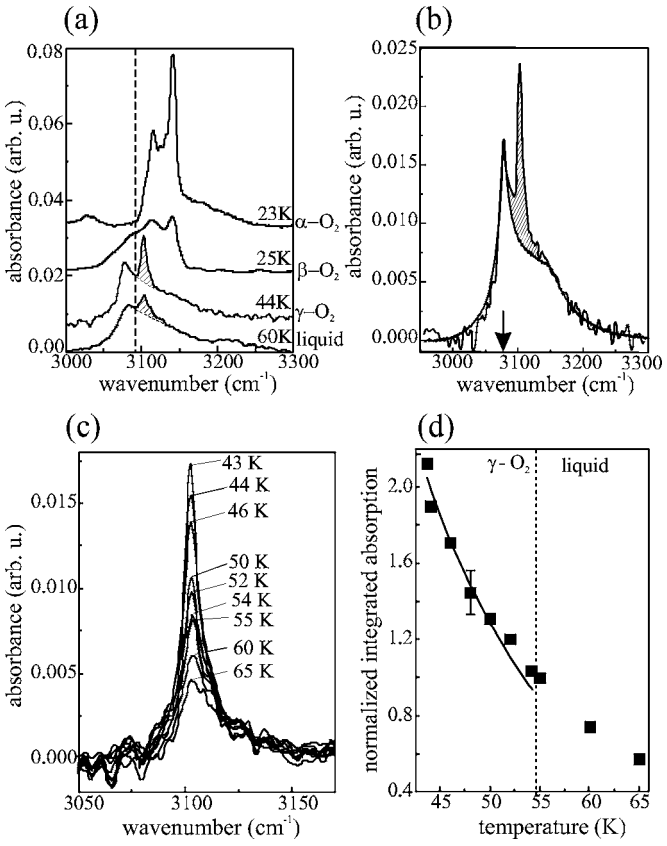

FIG. 9. Combined excitation spectrum in γ-O_2: (a) total spectrum as a function of temperature (band with shaded area of interest). (b) Spectrum at 44 K consisting out of phonon sideband to (0-2) overtone at 3070 cm^{-1} and (0-1)(0-1) combined vibration (shaded area). (c) Part of spectrum [shaded area of Fig. 9(b) as a function of temperature]. (d) Normalized integrated intensity $I(T)/I(55\ \mathrm{K})$ as a function of temperature in γ-O_2 and l-O_2. Considering magnetic interaction including thermal behavior is represented by solid line.

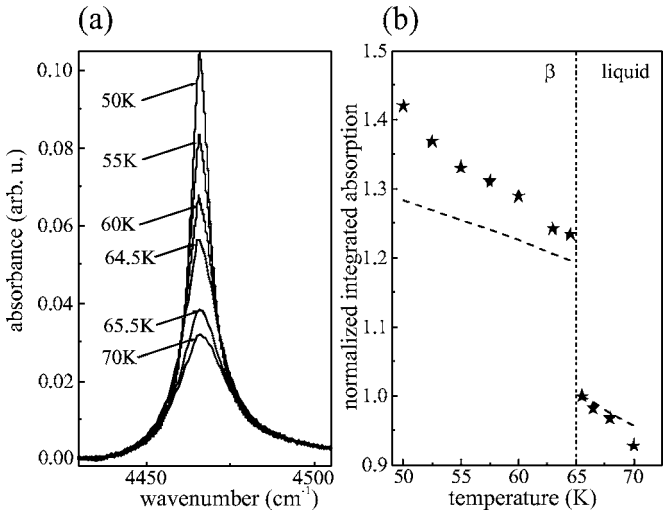

FIG. 10. (a) Combined excitation [(0-1)N_2(0-1)CO] spectrum in mixture $(N_2)_{0.59}$-$(CO)_{0.41}$ as a function of temperature. (b) Normalized integrated intensity $I(T)/I(65\ \mathrm{K})$ as a function of temperature in β^*-N_2-CO and l-phase. Considering thermal expansion by Ref. 4 as dashed line.

IR intensity, is proportional to the exchange interaction J_{dd} and the spin correlation function $\langle S_d S_d \rangle$

$$I(\mathrm{T}) \sim M_{dd}^2 \sim J_{dd}^2 \langle S_d S_d \rangle^2.$$

Using an exponential dependence of this exchange parameter J on intermolecular distance $R(T)$ including thermal expansion and the expression for $\langle \mathrm{S}_d \mathrm{S}_d \rangle$,[24] we can analyze the temperature dependence of the band intensity; the agreement between experimental data points and calculated dependence [the solid line in Fig. 9(d)] is excellent.

This absorption band persists also in the liquid phase and the temperature dependence of this absorption intensity shows no discontinuity at the melting point ($T \sim 55$ K). This means first, that the chainlike structure also persists in the l-O_2 (at least as short range order) and second, that the nearest-neighbor distance within chains does not change significantly at the melting point. (This aspect was already discussed by us in Ref. 25.)

3. Combined vibration (0-1)(0-1) in β^* N_2-CO

In this last section, we report the influence of foreign, but quasi-identical, molecules on the short range order parameter. Figure 10(a) shows a broad band around 4460 cm^{-1}. We varied both the temperature and the concentration [$(N_2)_{0.91}$-$(CO)_{0.09}$ and $(N_2)_{0.59}$-$(CO)_{0.41}$ and $(N_2)_{0.19}$-$(CO)_{0.81}$]. Due to this high doping by foreign molecules, we would not expect a strong phonon sideband perturbing this broad band, as occurs in the case of pure β-N_2 [Fig. 8(b)] or of pure γ-O_2 [Fig. 9(b)].

Figure 10(a) shows the temperature dependence of this absorption band; changes in band frequency and bandwidth are relatively small during heating but the change in band intensity is dramatic. The bandwidth here in β^* $(N_2)_{0.59}$-$(CO)_{0.41}$ is about 10 cm^{-1}, as in the pure case. The band maximum at 4466 cm^{-1} (T=50 K) can be modeled by the sum of the N_2 vibration (Raman-active A_g mode at 2326.5 cm^{-1} at 50 K) and of the CO vibration (IR-active mode at 2139 cm^{-1}).

We model this absorption band as in the former cases of the orientational disordered phases: two neighboring molecules of N_2 and CO, interacting via the electric quadrupole moment Q (N_2) and the electric dipole moment D (CO), are simultaneously excited to (0-1), vibrating out of phase; this combined excitation is a local excitation. Different pairs of molecules in different geometrical correlations are vibrating, producing the relatively large bandwidth (10 cm^{-1}) compared to the narrow vibron zone (1–2 cm^{-1}) in ordered systems.

In Fig. 10(b) we plot the intensity scaled at T=65 K, i.e., $I(T)/I(65\ \mathrm{K})$. This ratio decreases gradually with increasing temperature in β^*-$(N_2)_{0.59}$-$(CO)_{0.41}$ as well as in the liquid phase. There occurs a clear discontinuity at the melting point ($T_{\beta l}$). We express the integrated intensity as

$$I(T) \sim \rho^2 \cdot F(\mathbf{r}_i, \mathbf{r}_j),$$

where ρ is the density and the function $F(\mathbf{r}_i, \mathbf{r}_j)$ describes the strength of the orientational correlation between CO and N_2 molecules. The normalized density ρ^2 is plotted as a broken line in Fig. 10(b) [because the mixture N_2-CO is ideal and behaves like pure N_2 with this respect, we used data $R(T)$ from pure N_2]. The temperature behavior in the liquid N_2-CO is properly modeled, whereas the discrepancy between the experimental data and the theory (the broken line) increases during cooling but is much less pronounced than in pure N_2. This means that the admixing of CO, with its strong CO or OC orientation due to electrostatic dipole moment, suppresses the orientational correlation between N_2-N_2 molecules.

4. Comparison of systems

We studied the combined excitation (0-1)(0-1) of vibrating neighboring molecules in three systems (β-N_2, $\beta^*$$N_2$-CO, and γ-O_2). Especially noteworthy are comparisons of the integrated intensity $I(T)$, as a measure of molecule-molecule interaction, and the bandwidth $\Gamma(T)$, as a measure of inhomogeneous broadening due to disorder.

Because β-CO is similar to β-N_2 we would expect a similar combined vibration (0-1)(0-1) around 4270–4280 cm^{-1} [ν_0(IR)=2139 cm^{-1} at 50 K]. But the (0-2) transition (at 4250 cm^{-1}) is IR active. We observe this as a strong peak; its intensity is so large that the detector is saturated [Fig. 5(a)]. Although we can identify in that spectrum an asymmetry to the higher energetic side, it is not possible to deconvolute this strong peak into two excitations, i.e., (0-2) and (0-1)(0-1) vibrations. In addition the (0-2) excitation is broadened at the phase transition from α-CO ($\Gamma \sim 10$ cm^{-1}) to β-CO ($\Gamma > 30$ cm^{-1}).

The bandwidth or the basis width in ordered systems [see, e.g., Fig. 3(a)] is about 1–2 cm^{-1} for N_2, CO, and mixtures, and is about 6 cm^{-1} for oxygen. Here in a disordered system we find a bandwidth of about 10 cm^{-1} in the low temperature regime of each phase (35 K in β-N_2, 45 K in γ-O_2, and 50 K in N_2-CO). We attribute this to the (static) disorder due to

molecule geometry and molecule environment. An increase of temperature within these disordered phases causes a large increase in the bandwidth: in β-N_2, the bandwidth increases from $\Gamma=10\ cm^{-1}$ at 35 K to $\Gamma=50\ cm^{-1}$ at 60 K; in β^*-N_2-CO it changes from $\Gamma=6\ cm^{-1}$ at 50 K to $\Gamma=20\ cm^{-1}$ at 70 K; in γ-O_2 it increases from $\Gamma=10\ cm^{-1}$ at 45 K to $\Gamma=15\ cm^{-1}$ at 60 K. This inhomogeneous broadening is described by a dynamic disorder due to mode coupling of vibrations and translations/rotations. The effect is stronger for β-N_2 because of its anharmonicity of the large thermal amplitude.

The integrated band intensity $I(T)$ for this excitation is proportional to the short range order parameter and the specific interaction between neighboring molecules, by which a dipole moment is induced. In our diagrams [see Figs. 8(d), 9(d), and 10(b)], we normalized the integrated band intensity $I(T)/I(T^*)=1$ at a characteristic temperature T^* (the solid-liquid phase transition: in N_2, $T^*=64$ K; in O_2, $T^*=55$ K; and in N_2-CO, $T^*=65$ K). The normalized integrated intensity in β-N_2 decreases from 3 to 1 as the temperature increases in that phase. We were able to model this temperature dependence $I(T)$ either by the temperature dependence of the specific interaction [electric quadrupole moment and $R(T)$] or by a correlation function $F(r_{ij})$; both terms have the same weight [Fig. 8(d)]. In the mixture N_2-CO $I(T)$ decreases from 1.4 to 1 as the temperature increases in that phase. We modeled $I(T)$ either by the temperature dependence of the specific interaction [electrostatic dipole-quadrupole and $R(T)$] or the correlation function. In that case the ordering term (electrostatic dipole-quadrupole) has a stronger weight [Fig. 10(b)]. In γ-O_2, $I(T)$ decreases from 2 to 1 with increasing temperature in that phase. This variation can be completely modeled by the temperature dependence of the specific interaction (the magnetic interaction between disklike molecules).

The solid-liquid phase transition shows a clear jump in $I(T)$ for β-N_2 and for the N_2-CO mixture due to a jump in volume, but there is no change in $I(T)$ for γ-*l* O_2.

IV. CONCLUSION

We studied the temperature and concentration dependence of very weak absorption bands lying in the mid IR region of first ($2\ \nu_0$) and second ($3\ \nu_0$) overtones (systems of solid N_2, O_2, and CO, and mixtures of N_2-CO). From spectral fingerprints (band position, width, intensity, and shape), and on the basis of an unambiguous assignment, we determined the vibron DOS, modeled long and short range order parameters, and described static and dynamic disorder. We investigated ordered phases at low temperatures and orientationally disordered phases at higher temperatures. IR activity is induced in a molecule when neighboring molecules interact and vibrate simultaneously out of phase, as occurs with the (0-1)(0-1) excitation. We grew large polycrystalline samples with good optical as well as thermodynamic stable quality.

To model the long range order parameter $\eta(T)$ in ordered systems, it was sufficient to choose the specific molecular interaction (electric quadrupole moments in N_2, electric dipoles in CO and magnetic moments in O_2) and the proper temperature dependence of molecule-molecule distance $R(T)$. To model the short range order parameter $\eta(T)$ in disordered systems, we had to consider two effects: the temperature-dependent specific interaction and a temperature-dependent correlation function. Our spectroscopically derived values for the order parameter are in excellent agreement with previous results when such results are available, such as by x-ray Bragg scattering or by NQR data.

The order parameter in mixtures $\eta(T,c)$ has not been modeled theoretically, but for mixtures it is expected to lie between the two cases of pure systems.

We extended our studies also to the liquid phase in all four systems; we found similarities and discrepancies between plastic and liquid phases.

ACKNOWLEDGMENTS

This work was supported by Deutsche Forschungsgemeinschaft (Grant No. JO 86/10 and No. JO 86/11). We would like to thank Bruce W. Shore for helpful discussion on physics and for improving the readability of our manuscript.

[1] *Physics of Cryocrystals*, edited by V. G. Manzhelii and Yu. A. Freiman (AIP, Woodbury, New York, 1997).
[2] A. A. Freiman and H. J. Jodl, Phys. Rep. **401**, 1 (2004).
[3] A. P. Brodyanski, S. A. Medvedev, M. Vetter, J. Kreutz, and H. J. Jodl, Phys. Rev. B **66**, 104301 (2002).
[4] T. A. Scott, Phys. Lett., C **27C**, 89 (1976).
[5] N. Legay-Sommaire and F. Legay, Chem. Phys. **66**, 315 (1982).
[6] G. Zumofen, J. Chem. Phys. **68**, 3747 (1978).
[7] W. M. Grundy, B. Schmitt, and E. Quirico, Icarus **105**, 254 (1993).
[8] F. Legay and N. Legay-Sommaire, Chem. Phys. **206**, 367 (1996).
[9] F. Legay and N. Legay-Sommaire, Chem. Phys. **65**, 49 (1982).
[10] M. Minenko, M. Vetter, A. P. Brodyanski, and H. J. Jodl, Fiz. Nizk. Temp. **26**, 947 (2000) [Low Temp. Phys. **26**, 699 (2000)].
[11] H. Dubost, Chem. Phys. **12**, 139 (1976).
[12] R. D. Beck, M. F. Hineman, and J. W. Nibler, J. Chem. Phys. **92**, 7068 (1990).
[13] R. Quillon, C. Turc, J. P. Lemaistre, and P. Ranson, J. Chem. Phys. **93**, 3005 (1990).
[14] T. N. Antsygina, V. A. Slusarev, Yu. A. Freiman, and A. I. Erenburg, J. Low Temp. Phys. **56**, 331 (1984).
[15] M. A. Strzhemechny, J. Low Temp. Phys. **139**, 581 (2005).
[16] G. Herzberg, *Molecular Spectra and Molecular Structure I. Spectra of Diatomic Molecules* (Van Nostrand Reinhold Company, New York, 1950).
[17] F. Log, J. L. Brookeman, A. Rigamonti, and T. Scott, J. Chem. Phys. **74**, 3120 (1981).
[18] K. R. Witters and J. E. Cahill, J. Chem. Phys. **67**, 2405 (1977).

[19] I. Y. Fugol, L. V. Khachchina, and I. M. Pritula, Sov. J. Low Temp. Phys. **13**, 102 (1987).
[20] M. J. Angwin and J. Wasserman, J. Chem. Phys. **44**, 417 (1966).
[21] S. Medevedev, M. Santoro, F. Gorelli, Y. Gaididei, V. Loktev, and H. J. Jodl, J. Phys. Chem. B **107**, 4768 (2003).
[22] S. Medvedev, J. Kreutz, and H. Jodl, J. Phys.: Condens. Matter **15**, 7375 (2003).
[23] A. v. d. Avoird, W. J. Briels, and A. P. Jansen, J. Chem. Phys. **81**, 3658 (1984).
[24] A. P. Brodyanski, Y. Freiman, and A. Jezowski, J. Phys.: Condens. Matter **1**, 999 (1989).
[25] A. Brodyanski, S. Medvedev, M. Minenko, and H. J. Jodl, in *Frontiers of High-Pressure Research II: Application of High Pressure to Low-Dimensional Novel Electronic Materials*, edited by H. D. Hochheimer, B. Kuchta, P. K. Dorhout, and J. L. Yarger, NATO Science Series (Kluwer Academic Publishers, Dordrecht, 2001), pp. 217–234.